Tampereen yliopisto

Jenni Keränen

OPTIMIZATION OF CALCIUM IMAGING FOR HUMAN EMBRYONIC STEM CELL-DERIVED RETINAL PIGMENT EPITHELIUM IN CELL CULTURE CONDITIONS

Faculty of Medicine and Health Technology (MET)
Bachelor's thesis
April 2021

TIIVISTELMÄ

Jenni Keränen: Kalsiumkuvantamisen optimointi ihmisen alkion kantasoluista erilaistetuille verkkokalvon pigmenttiepiteelisoluille soluviljelyolosuhteissa
Kandidaatin tutkielma
Tampereen yliopisto
Bioteknologian tutkinto-ohjelma
Huhtikuu 2021

Verkkokalvon pigmenttiepiteeli (engl. retinal pigment epithelium, RPE) on kuusikulmaisista soluista koostuva yksinkertainen epiteelisolukerros, joka sijaitsee silmän takaosassa näköaistisolujen ulkojäsenten ja suonikalvon välissä. RPE on elintärkeä näköaistisolujen ja siten koko optisen järjestelmän selviytymiselle, koska sillä on tärkeä rooli esimerkiksi verkkokalvon ravinteiden kuljetuksessa, foto-oksidatiivisen stressin vähentämisessä ja verkkokalvon ionitasapainon ylläpidossa.

Kalsiumionit (Ca^{2+}) ovat yksi merkittävimmistä signalointimolekyyleistä, joita esiintyy eläinsoluissa. Monia tärkeitä soluprosesseja, kuten solunjakautumista ja solukuolemaa, ohjataan monimutkaisten Ca^{2+}-signalointireittien välityksellä. RPE:ssä Ca^{2+} varastoidaan pääasiassa endoplasmakalvostoon ja voimakkaasti pigmentoituneihin melanosomeihin, joista ionit voidaan vapauttaa esimerkiksi jännite- tai ligandiriippuvaisten ionikanavien avulla.

Elävissä soluissa vapaata sytosolista Ca^{2+} voidaan mitata optisesti Ca^{2+}-kuvantamiseksi kutsutun tekniikan avulla. Tässä työssä Ca^{2+}-kuvantaminen suoritettiin fluoresenssimikroskopialla ja kemiallisella Ca^{2+}-indikaattorilla, Fluo-4:llä. Kun Fluo-4 sitoutuu sytosoliin vapautuneeseen Ca^{2+}:iin, Fluo-4:n fluoresenssi-intensiteetissä tapahtuu muutos, joka voidaan havaita fluoresenssimikroskoopilla.

Ca^{2+}-kuvantamiskokeet toteutetaan usein huoneenlämmössä, vaikka elävien solujen optimaalinen lämpötila on +37°C. Tämän tutkielman tarkoituksena oli optimoida Ca^{2+}-kuvantamismenetelmää RPE:lle soluviljelyolosuhteissa, koska solujen kuvantaminen mahdollisimman lähellä niiden fysiologisia olosuhteita voi johtaa parempiin tuloksiin verrattuna huoneenlämmössä toteutettuun kuvantamiseen. Tässä tutkimuksessa käytetyt solut olivat ihmisen alkion kantasoluista peräisin olevia Regea08/023 solulinjasta erilaistettuja RPE-soluja. Regea08/017 linjan soluista erilaistettuja RPE-soluja käytettiin kontrollina. Optimointia varten valittiin kaksi erilaista Ca^{2+}-kuvantamisliuosta testattavaksi huoneenlämpötilassa ja +37°C:ssa toteutetuille Ca^{2+}-kuvantamisille: Elliot-suolaliuos ja Hibernate™-A-solujen kasvatusliuos.

Ca^{2+}-kuvantamisen lisäksi suoritettiin immunovärjäys konfokaalikuvantamista varten $Ca_V1.3$-jännitekytkettyjen Ca^{2+}-kanavien läsnäolon osoittamiseksi. $Ca_V1.3$:n lisäksi soluista värjättiin tiivisliitoksiin sitoutuva proteiini ZO-1. Solutukirangan aktiini värjättiin aktiiniin sitoutuvalla myrkyllä, falloidiinilla.

Suunniteltuja Ca^{2+}-kuvantamiskokeita ei voitu suorittaa mahdollisesti liian vanhojen 08/023 solulinjan solujen ja vanhentuneen Fluo-4:n vuoksi. Ensimmäisten Elliot ja Hibernate-huoneenlämpökuvausten jälkeen Ca^{2+}-kuvantamisdataa ei saatu mistään näytteessä. Hibernate-kasvatusliuos ei soveltunut fluoresenssimikroskoopilla toteutettuun Ca^{2+}-kuvantamiseen, koska se aiheutti paljon häiritsevää taustafluoresenssia kuvantamisen aikana. Jotta voidaan todella arvioida, miten soluviljelyolosuhteissa toteutettu Ca^{2+}- kuvantaminen vaikuttaa kuvantamistuloksiin, tulisi kokeet toistaa nuoremmilla soluilla sekä uudella Fluo-4-liuoksella.

Avainsanat: verkkokalvon pigmenttiepiteeli, hESC-RPE, Ca^{2+}-signalointi, Ca^{2+}-kuvantaminen

ABSTRACT

Jenni Keränen: Optimization of calcium imaging for human embryonic stem cell-derived retinal pigment epithelium in cell culture conditions
Bachelor's thesis
Tampere University
Degree Programme in Biotechnology
April 2021

Retinal pigment epithelium (RPE) is a monolayer of hexagonal cells located at the back of the eye between the outer segments of the photoreceptors and the choriocapillaris. RPE is vital for the survival of the photoreceptors and the whole optical system due to its role in, for example, nutrient transport, photo-oxidative stress reduction and ion homeostasis upkeep.

Calcium ions (Ca^{2+}) are one of the most significant signalling molecules present in animal cells. Important cellular processes such as cell division and cell death are controlled through complex Ca^{2+} signalling pathways. In RPE, Ca^{2+} is stored mainly in the endoplasmic reticulum and highly pigmented melanosomes, from where the ions can be released through voltage-gated ion channels or ligand-gated ion channels, for example.

In living cells, free cytosolic Ca^{2+} can be optically measured with a technique called Ca^{2+} imaging. In this thesis, Ca^{2+} imaging was conducted with a chemical fluorescence indicator Fluo-4 together combined with fluorescence microscopy. When Fluo-4 binds freed Ca^{2+} in the cytosol, a change in the fluorescence intensity of Fluo-4 occurs. This change can be detected and recorded with a fluorescence microscope, and thus the Ca^{2+} signalling of living cells can be studied.

Ca^{2+} imaging experiments are often conducted at RT, even though the optimal temperature for living cells is +37°C. Imaging cells closer to their physiological conditions could yield better results compared to imaging performed at RT. Therefore, this thesis aimed to optimize Ca^{2+} imaging for RPE in cell culture conditions. The cells used for this study were human embryonic stem cell-derived (hESC-derived) RPE cells differentiated from the Regea08/023 cell line. RPE cells differentiated from the Regea08/017 cell line were used as a cell control. Two different Ca^{2+} imaging solutions, Elliot salt solution and Hibernate™ -A cell nutrient medium, were chosen to be tested for Ca^{2+} imaging performed at RT and +37°C.

In addition to Ca^{2+} imaging, immunofluorescence staining was performed for confocal imaging to show the presence of $Ca_V1.3$ voltage-gated Ca^{2+} channels in the hESC-RPE cells. In addition to $Ca_V1.3$, the cells were stained for a tight-junction-binding protein ZO-1. Intracellular actin was stained with the actin-binding toxin phalloidin.

The planned Ca^{2+} imaging experiments could not be conducted due to possibly too old 08/023 cells and expired Fluo-4 stock. After the first imaging sessions with Elliot solution and Hibernate -medium at RT, no Ca^{2+} imaging data could be recorded from any of the samples. Hibernate -medium was deemed not suitable for Ca^{2+} imaging performed with fluorescence microscopy due to a high amount of disturbing background during imaging. To truly assess how Ca^{2+} imaging performed at +37°C instead of RT affects the results, the experiments should be repeated with younger cells and a new Fluo-4 stock.

Keywords: retinal pigment epithelium, hESC-RPE, Ca^{2+} signalling, Ca^{2+} imaging

ACKNOWLEDGEMENTS

This thesis is a part of my Bachelor of Science -degree at the Faculty of Medicine and Health Technology (MET) at Tampere University. The research work was conducted jointly at Docent Soile Nymark's and Academy Research Fellow, Docent Teemu Ihalainen's research groups. I thank the Biocenter Finland (BF) and Tampere Imaging Facility (TIF) for providing the equipment for Ca^{2+} and confocal imaging.

I would like to thank Dr. Nymark and Dr. Ihalainen, and the whole Biophysics of the Eye and Cellular Biophysics groups for the interesting research subject and materials necessary for conducting it. I would also like to thank my instructors MSc. Jenni Partinen and MSc. Sanna Korpela for their valuable guidance, assistance and reassurance throughout this thesis. Lastly, I would like to thank my friends and family for their support during the writing process.

Tampere, 21.4.2021

Jenni Keränen

CONTENTS

1. INTRODUCTION

Retinal pigment epithelium (RPE) is a monolayer of hexagonal cells that forms a part of the blood/retina barrier of the eye. RPE is located at the back of the eye between the outer segments of the photoreceptors and the choriocapillaris. As most epithelium, RPE is structurally heavily polarised. The apical membrane of the RPE has long microvilli -structures that form close interactions with the photoreceptor outer segments, while the basolateral membrane faces the Bruch's membrane that acts as a barrier between the RPE and the choriocapillaris. (Strauss 2005) As the name states, RPE is highly pigmented due to the presence of dark-coloured melanin stored in special cell organelles, called melanosomes (Lakkaraju et al. 2020). The pigmentation is important to the RPE's ability to absorb scattered light and thus reduce the photo-oxidative stress of the photoreceptors (Strauss 2005). In addition to absorbing scattered light, RPE has numerous other functions that maintain the viability and functionality of the photoreceptors. For example, RPE transports nutrients, ions and water between the photoreceptors and the choriocapillaris, as well as stabilizes the ion homeostasis in the subretinal space (Strauss 2005). In addition, RPE participates in the renewal process of the photoreceptors, which is crucial for their normal function and the formation of visual perception (Lakkaraju et al. 2020).

Calcium ions (Ca^{2+}) are one of the many important signalling molecules present in animal cells. Ca^{2+} signalling is used to control cellular processes such as cell contraction and division, cell migration, and cell death (Alberts et al. 2015). Ca^{2+} signalling is based on the rapid release of Ca^{2+} to the cell cytoplasm, which can be triggered by e.g., depolarization of the cell membrane or binding of intracellular messengers such as ATP or glutamate (Alberts et al. 2015). In spontaneous Ca^{2+} signalling, Ca^{2+} is released due to naturally occurring cell communication rather than a specific trigger. The flow of the ions is made possible by the steep difference in extracellular and intracellular Ca^{2+} ion concentrations (Alberts et al. 2015). The intracellular Ca^{2+} concentration can be as low as 100 nM, while during a Ca^{2+} influx the concentration can rise up to 1000 nM (Bootman 2012). The main routes for Ca^{2+} intake are from the extracellular space by protein channels located on the cell membrane, and from the intracellular Ca^{2+} storages (Abu Khamidakh 2019). The most significant Ca^{2+} storage in animal cells is the endoplasmic reticulum, but in RPE, the melanosomes can also store large amounts of Ca^{2+} (Salceda and Riesgo-Escovar 1990). In turn, ion channels such as voltage-gated Ca^{2+} channels (Ca_V), open and allow an influx of extracellular Ca^{2+} to occur across the cell membrane in response to membrane depolarization (Abu Khamidakh 2019). Ca_V channels include, for example, $Ca_V1.3$ localized at the apical membrane of RPE and $Ca_V3.1$ localized at the microvilli (Korkka et al. 2018). In addition to voltage-gated ion channels, ligand-gated ion channels

such as glutamate receptors take part in allowing extracellular Ca^{2+} to enter the cell (Kew and Kemp 2005).

Free cytosolic Ca^{2+} in the RPE can be optically measured with calcium imaging. In this thesis, Ca^{2+} imaging was conducted with an upright widefield fluorescent microscope and a chemical Ca^{2+} indicator Fluo-4-AM. ATP was used to trigger the release of Ca^{2+} from the intracellular Ca^{2+} storages. Chemical indicators, such as Fluo-4, are highly selective molecules that can bind certain ions. Fluo-4 selectively binds Ca^{2+}, which causes an increase in the fluorescence intensity of the Fluo-4 -molecules. This change can then be detected with a fluorescent microscope. (https://www.thermofisher.com/order/catalog/product/F14201#/F14201, 24.3.2021) The absorption maximum of Fluo-4 is at 494 nm and the emission maximum at 516 nm (Gee et al. 2000).

In addition to Ca^{2+} imaging, immunofluorescence staining was performed, and laser scanning confocal microscopy (LSCM) was used to show the presence of $Ca_V1.3$ channels in the RPE cells. Immunofluorescence staining utilizes antibodies along with fluorescent dyes to stain different proteins in the cells. In laser scanning confocal imaging, laser lights are used to scan the sample and excite the different fluorescent dyes in it. Due to the scanning process, light can be collected only from a single focal plane at a time. (https://www.microscopyu.com/techniques/confocal/introductory-confocal-concepts, 24.3.2021)

This thesis aimed to optimize Ca^{2+} imaging for human embryonic stem cell-derived RPE in cell culture conditions. +37°C is the physiological temperature for human cells, and thus, imaging the cells at +37°C could lead to improved Ca^{2+} imaging results compared to imaging performed at RT. For the optimization, two possible imaging solutions were chosen: Elliot salt solution and Hibernate™ -A cell nutrient medium (Gibco™, United States). Elliot solution is the solution mainly used for Ca^{2+} imaging at Dr. Nymark's laboratory, and therefore its suitability for +37°C imaging was chosen to be tested. Hibernate™ Medium was chosen due to its ability to maintain ambient CO_2 levels and consequently mimic the cell culture environment during the imaging process (https://www.thermofisher.com/order/catalog/product/A1247501#/A1247501, 23.3.2021).

2. MATERIALS AND METHODS

2.1 Cell culture

The human embryonic stem cell-derived retinal pigment epithelial cells (hESC-RPE cells) used in this thesis project were differentiated from the hESC cell lines Regea08/023 and Regea08/017. Both cell lines were derived and characterized from blastocyst-stage embryos at Professor Heli

Skottman's laboratory at Tampere University (Skottman 2010). The cells were differentiated, thawed and maturated at Dr. Nymark's laboratory before the start of this thesis project. During the experiments conducted for this thesis, the 08/023 cells were 14-15 weeks old. The 08/017 cells were 8 weeks old.

The cells were grown on 24-well plate transparent TC-inserts (Sarstedt, Germany) with 1 µm pores. The polyethylene terephthalate membranes of the inserts were coated at Dr. Nymark's laboratory with collagen IV from human placenta (Sigma-Aldrich, United States) and laminin 521 (Biolamina, Sweden). The final area density of the insert membranes was 10 µg/cm^2 for collagen IV and 1.8 µg/cm^2 for laminin 521.

The cells were cultured at +37°C in 5 % CO_2 in a culture medium consisting of KnockOUT™ Dulbecco's Modified Eagle's Medium (KO-DMEM) (Gibco™), 15 % KnockOUT™ Serum Replacement (KO-SR) (Gibco™), 2 mM GlutaMAX™ (Gibco™), 0.1 mM 2-mercaptoethanol (Gibco™), 1 % Minimum Essential Medium nonessential amino acids (Lonza, Switzerland) and 50 U/ml penicillin/streptomycin (Lonza). The culture medium was replenished three times a week on Mondays, Wednesdays and Fridays. 300 µl of the culture medium was added to the apical side and 700 µl to the basal side of the cells.

2.2 Immunofluorescence staining and confocal imaging

Prior to confocal imaging, the cells were stained for $Ca_V1.3$ and a tight junction protein ZO-1. Before staining, the cells were fixed in 4% PFA-PBS (15 minutes at RT) and permeabilized in 0.1% Triton-X-100-PBS (15 minutes at RT). 3% BSA-PBS was used for blocking (1h at RT). Both primary and secondary antibody dilutions were prepared in 3% BSA-PBS. See Table 1 for the antibodies used. Primary antibodies were incubated for 1h at RT. After PBS washes, secondary antibodies were added together with phalloidin (643 nm) (ATTO-TEC, Germany) and the samples were incubated for 1h at RT in the dark.

Table 1: Primary and secondary antibody details. *Used primary and secondary antibodies, their manufacturers and dilutions. 1:100 dilution of phalloidin was added together with the secondary antibodies.*

	Antibody	**Manufacturer**	**Dilution**
Primary antibodies	Anti-$Ca_V1.3$, rabbit	Alomone labs, Israel	1:100
	Anti-ZO-1, mouse	Invitrogen™, United States	1:50
Secondary antibodies	Goat anti-rabbit IgG, Alexa Fluor 488 nm	Invitrogen™	1:200
	Goat anti-mouse IgG, Alexa Fluor 568 nm	Invitrogen™	1:200

The stained cells were imaged with the Zeiss LSM 800 laser scanning confocal microscope at Tampere Imaging Facility (Tampere University). Imaging was performed with the Zeiss Plan-Apochromat 63x/1.40 oil immersion objective. Voxel size was set to x = y = 100 nm and z = 150 nm. 1024 x 1024 pixel stacks were acquired with a line average of 2. The images were saved in .czi format and processed with ImageJ. The images were filtered with Gaussian blur and the pixel intensities were modified with only linear contrast and brightness adjustments.

2.3 Calcium imaging

Before imaging, the cells were loaded with the Fluo-4-AM Ca^{2+} indicator. (Molecular Probes™, United States). 4 µl of Fluo-4 dissolved into DMSO (1 mM) was added to 1 ml of the loading solution (see Table 2). The final concentration of Fluo-4-AM in the loading solution was 4 µM. 300 µl of the prepared Fluo-4 solution was added to the apical and 700 µl to the basal side of the cells. The samples were incubated for 45 minutes at RT in the dark, after which the samples were washed three times with the loading solution (see Table 2) with a 5-minute incubation each wash. During the loading processes with Elliot solution, parts of the cell layer began to break down and detach for unknown reasons. All the samples had enough intact areas for finishing the imaging experiments. The numbers in brackets in Table 2 indicate two different samples imaged in those imaging conditions.

Table 2: Loading and imaging solutions and imaging temperatures chosen for the experiment. *Elliot RT, Hibernate RT and Elliot +37°C samples were from the 08/023 cell line. 017 control was from the 08/017 cell line. The numbers in brackets indicate that imaging was performed with two different samples in those imaging conditions. pH and osmolarity were adjusted separately for the RT and +37°C Elliot solutions.*

Sample	Loading solution	Imaging solution	Imaging temp.
Elliot RT (1, 2)	Elliot solution, RT	Elliot solution, RT	RT
Hibernate RT	Hibernate -medium	Hibernate -medium	RT
Elliot +37°C (1, 2)	Elliot solution, 37°C	Elliot solution, +37°C	+37°C
017 control	Elliot solution, RT	Elliot solution, RT	RT

Elliot solution was prepared from 1 M salt solutions and Milli-Q H_2O. In the final solution the concentrations of the salt solutions were as follows: NaCl 137 mM, KCl 5 mM, KH_2PO_4 0.44 mM, HEPES 20 mM, $NaHCO_3$ 4.2 mM, glucose 5 mM, $MgCl_2$ 1.2 mM and $CaCl_2$ 2 mM. The pH of the Elliot solution was adjusted to 7.4 with NaOH and the osmolarity to 330 mOsm with sucrose with

the Gonotec Osmomat 030 (Labo Line Oy, Finland). Both the pH and osmolarity were adjusted separately for the RT and +37°C Elliot solutions.

Ca^{2+} imaging was performed with the Nikon Eclipse FN1 upright fluorescence microscope at Tampere Imaging Facility with the Nikon CFI Apo LWD 25x/1.1 water dipping objective. Pixel size was set to x = y = 520 nm and 1024 x 1024 pixel images were acquired. The membrane with loaded cells was cut from the insert with a scalpel and placed on a 5 cm plate with the apical side facing up. The cut membrane was secured on the plate with an anchor fastened with silicone paste. 10 ml of imaging solution was carefully added on top of the cells and the plate was placed in the imaging chamber. When imaging at +37°C, the objective was warmed up to +40.5°C, and the imaging chamber to +38.5°C to ensure the imaging solution and thus the cells were kept at +37°C for the full duration of the imaging.

During the imaging, the excitation wavelength used for Fluo-4 was 488nm. Three 1-minute time-lapses from three different locations on the sample were taken to observe the spontaneous Ca^{2+} activity of the cells. In addition, the ATP response of the cells was studied. For this, a 10-minute time-lapse from the third location was taken from each sample. During the 10-minute time-lapse, 200 µl of 5 µM Na^{+} -ATP solution (Sigma-Aldrich) prepared in the imaging solution was pipetted to the plate at the 1-minute time point. The final concentration of ATP on the plate was 100 µM.

In addition to the 08/023 cells, one 08/017 cell line sample was imaged as a control. The cells were prepared as the 08/023 cells. During imaging, perfusion was used with Elliot solution and 100 µM Na+ -ATP solution.

The Ca^{2+} imaging footage was saved in .nd2 format and processed with ImageJ by plotting intensity plots. For spontaneous signalling, the intensity plots were plotted for a single cell to make sure the possible detected change in fluorescence could be captured. For ATP responses, a selected area from the footage was chosen for the intensity plots. Bleaching of the images was not corrected because photobleaching did not change the outcome of the results, and bleach correction in ImageJ would have reduced the recorded ATP response intensity spikes. For the photo series in both cases, pixel intensities were modified with linear brightness adjustments after intensity plots had been plotted.

3. RESULTS

3.1 Confocal imaging

Cells from the 08/023 cell line were stained for confocal imaging to show the presence of $Ca_V1.3$ in the samples. The $Ca_V1.3$ channels alongside the tight junction protein ZO-1, and intracellular actin stained with phalloidin can be seen in Figure 1.

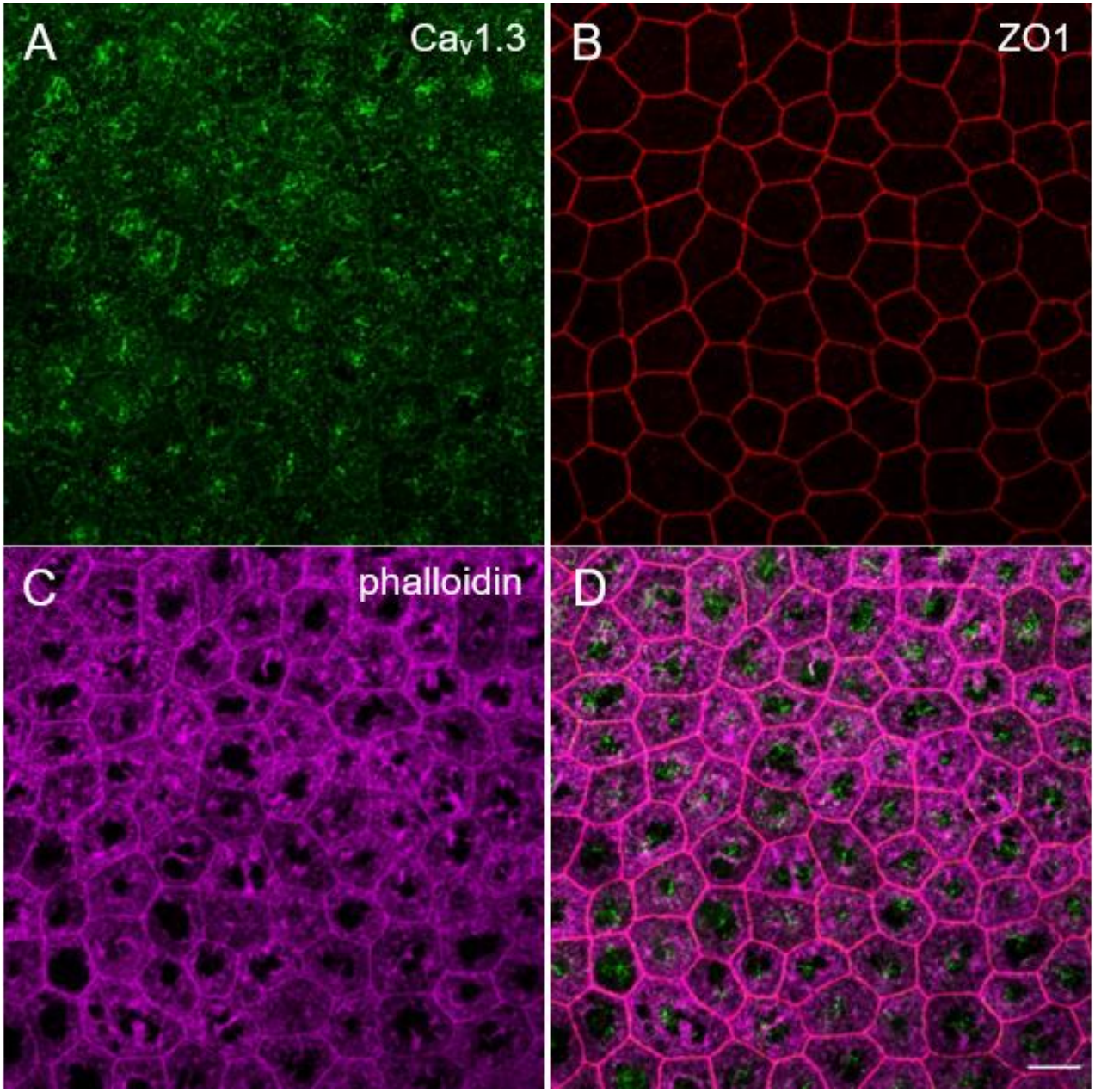

Figure 1: Maximum intensity projections (MIP) of 08/023 hESC-RPE cells. *$Ca_V1.3$ voltage-gated Ca^{2+} channels were stained for 488 nm (A), ZO-1 tight junction proteins for 568 nm (B) and actin-binding phalloidin for 643 nm (C). All three channels are merged in (D). The images' sizes are 1024 x 1024 pixels. The scale bar is 10 µm.*

3.2 Calcium imaging: spontaneous signalling

Both spontaneous Ca^{2+} signalling and ATP responses were recorded with Ca^{2+} imaging in different imaging conditions. Since the emphasis is on the ATP responses, only examples of spontaneous Ca^{2+} signalling are shown below with series of fluorescence images and intensity plots. Spontaneous signalling was imaged for 60 s from three different locations on the sample. The images and plots are from the first location for each sample. Figure 2 shows spontaneous signalling in the Elliot RT 1 -sample (see Table 2), Figure 3 shows the spontaneous signalling in the Hibernate RT -sample, and Figure 4 shows the lack of signalling in the Elliot +37°C 1 -sample. In the Elliot RT 1 -sample, a spike in the intensity can be seen at 10.5 s. In Hibernate RT, no clear intensity spike can be seen from the plot, but a change in the fluorescence of the cell can be visually detected. No spontaneous Ca^{2+} signalling was observed in the Elliot +37°C samples or the 017 control sample.

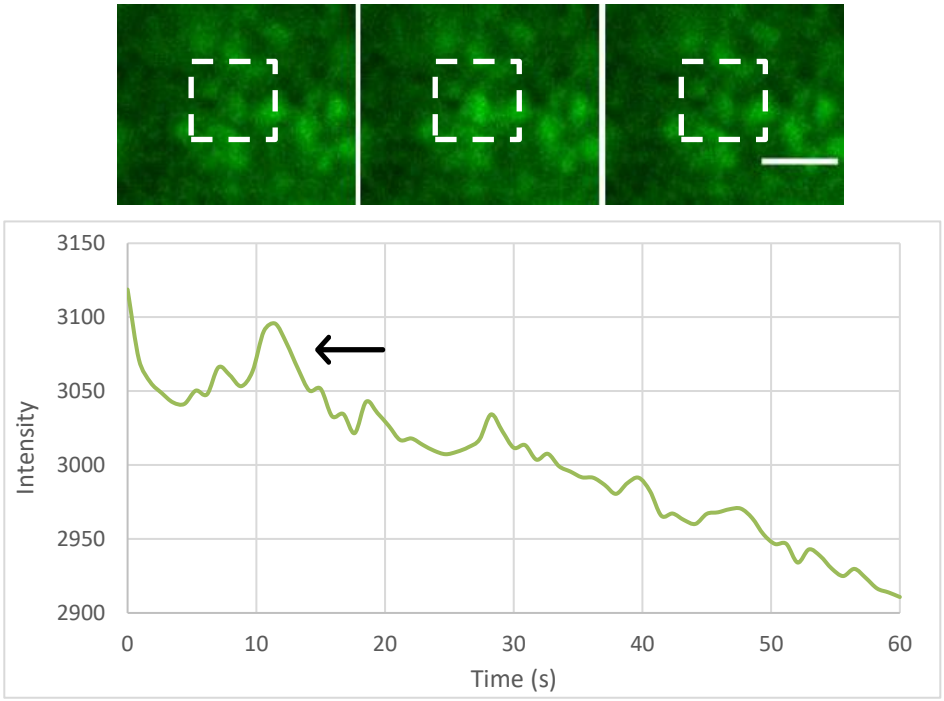

Figure 2: Spontaneous signalling of a single cell from the Elliot RT 1 -sample. *Spontaneous signalling was imaged for 60 s. A series of fluorescence images (time points: 8.8 s, 10.5 s, 15.8 s) showing the change in fluorescence of a single cell during spontaneous Ca^{2+} signalling, and an intensity plot of the single cell's intensity changes. The intensity spike marked on the plot (arrow) corresponds with the increase of fluorescence seen in the marked cell (dashed lines) in the series of images. The cropped images' sizes are 67 x 66 pixels. The scale bar size is 20 µm.*

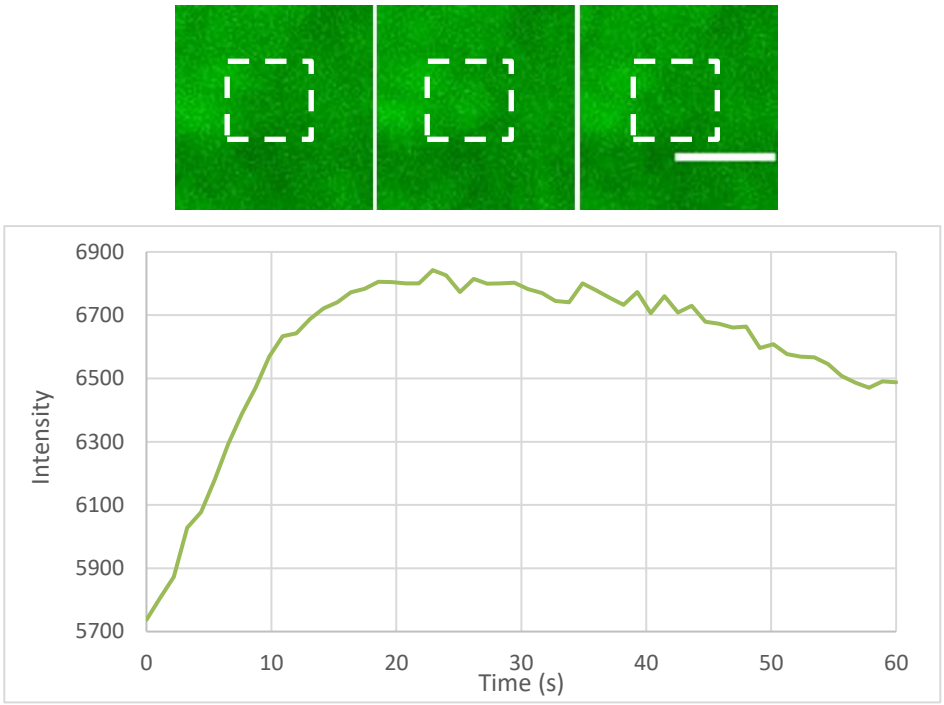

Figure 3: Spontaneous signalling of a single cell from the Hibernate RT -sample. *Spontaneous signalling was imaged for 60 s. A series of fluorescence images (time points: 41.5 s, 42.5 s, 47.0 s) showing the increase and decrease in fluorescence of a single marked cell during spontaneous Ca^{2+} signalling, and an intensity plot of the single cell's spontaneous signalling. The cropped images' sizes are 75 x 78 pixels. The scale bar size is 20 µm.*

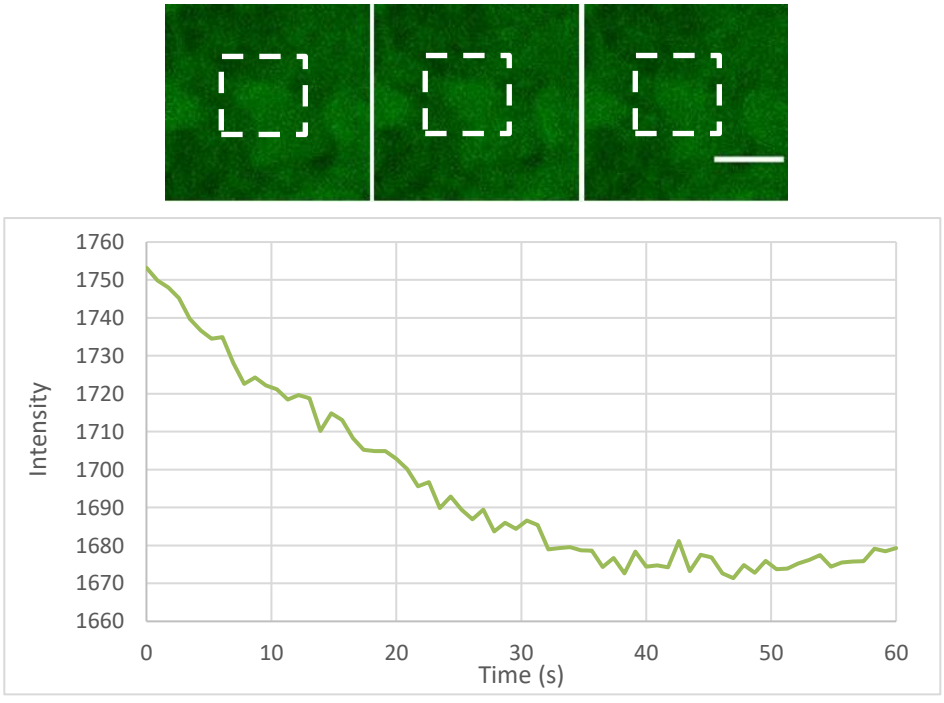

Figure 4: Spontaneous signalling of a single cell from the Elliot +37°C 1 -sample. *Spontaneous signalling was imaged for 60 s. A series of fluorescence images (time points: 58.2 s, 59.1 s, 60 s) and an intensity plot of a single cell showing no observed spontaneous signalling. The cropped images' sizes are 112 x 107 pixels. The scale bar size is 20 µm.*

3.3 Calcium imaging: ATP response

ATP was added to the samples because ATP binding to its receptors in the cell triggers a release of Ca^{2+} from the intracellular Ca^{2+} storages. As with spontaneous Ca^{2+} signalling, examples of the ATP responses are also shown with series of fluorescence images and intensity plots. All ATP responses are listed in Table 3 in the order the samples were imaged. In Figure 5, the ATP response of a selected area from the Elliot RT 1 -sample is shown alongside its intensity plot. The increase in intensity due to the ATP response can be seen at the 65.4 s time point, after which it immediately begins to decrease. The ATP response of a selected area from the Hibernate RT sample is shown in Figure 6. No change in the sample's fluorescence can be visually detected, but the intensity plot shows a rapid increase in intensity at 261 s followed by an immediate decrease.

No clear ATP response could be recorded from Elliot RT 2, Elliot +37°C 1 and 2, and 017 control -samples, thus no examples of them are shown below.

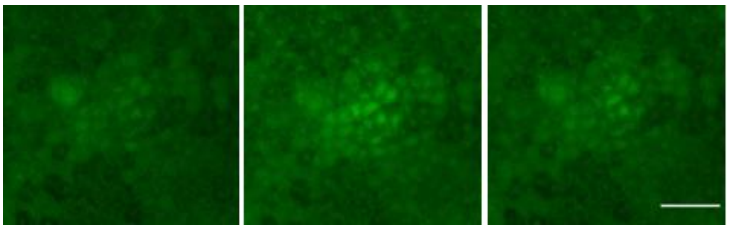

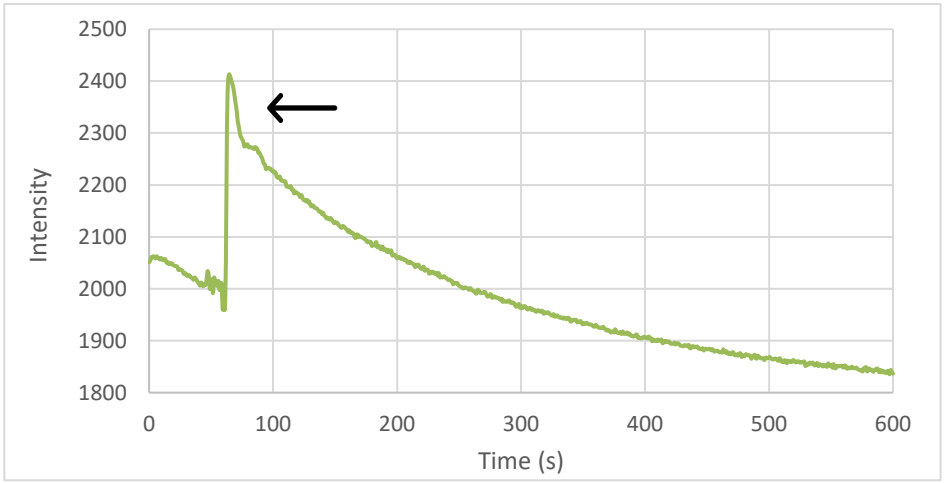

Figure 5: ATP response in the Elliot RT 1 -sample. *Ca^{2+} signalling during an ATP response was imaged for 600 s. A series of fluorescence images (time points: 61.0 s, 65.4 s, 143.9 s) showing the increase and decrease in fluorescence of a selected area during an ATP response, and an intensity plot that shows the intensity change during the response. The intensity spike marked on the plot (arrow) corresponds with the increase of fluorescence in the series of images. The cropped images' sizes are 305 x 286 pixels. The scale bar size is 40 µm.*

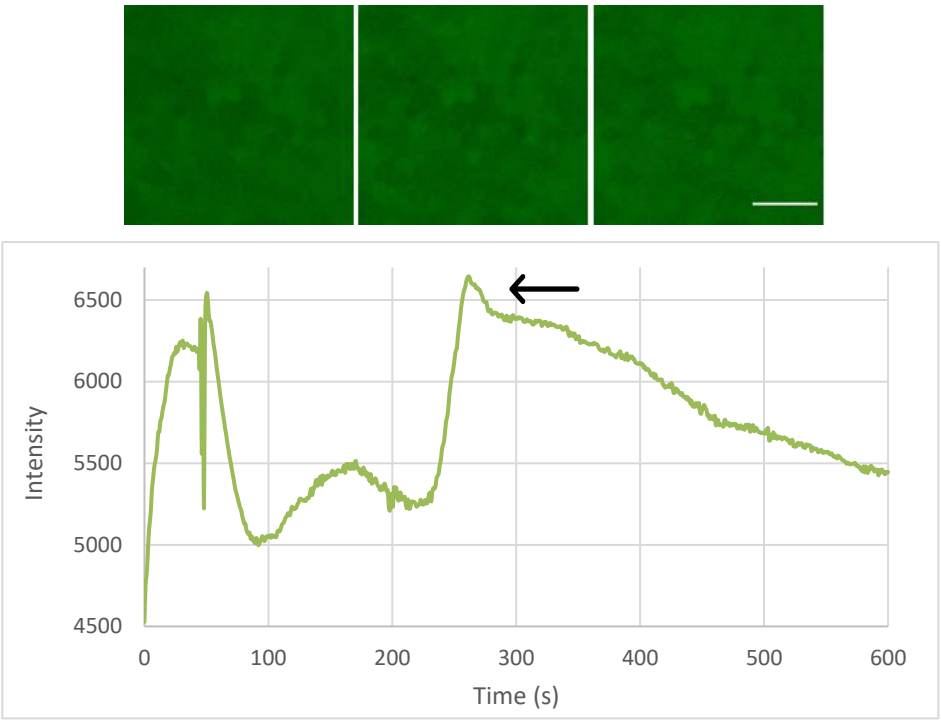

Figure 6: ATP response in the Hibernate RT -sample. *Ca^{2+} signalling during an ATP response was imaged for 600 s. A series of fluorescence images (time points: 246.0 s, 261.4 s, 336.9 s) from a selected area, and an intensity plot of the area's ATP response. The ATP response is marked in the plot (arrow). The cropped images' sizes are 269 x 260 pixels. The scale bar size is 40 µm.*

All the recorded ATP response spikes and the relative intensities at the ATP response spike peaks can be seen in Table 3. The relative intensities were calculated by dividing the intensity value at 0 s by the intensity value at the ATP response spike peak and subtracting the result from one. The samples are listed in their imaging order. For Elliot RT 1, the relative intensity at the ATP response spike peak at 65.4 s was 14.50 % and for Hibernate RT at 261.43 s 31.87 %. No proper ATP response could be recorded from the rest of the samples.

Table 3: ATP responses of all samples in their imaging order. *All available ATP responses are listed below by presenting their relative intensities at the ATP response spike peak. The samples are listed in their imaging order.*

Sample	Intensity at 0 s	Relative intensity at 60 s	ATP response spike peak	Relative intensity at ATP response spike peak
Elliot RT 1	2051.09	-4.29 %	65.4 s	14.50 %
Hibernate RT	4527.82	24.39 %	261.43 s	31.87 %
Elliot +37°C 1	1648.39	0.61 %	-	-
Elliot +37°C 2	2136.58	0,52 %	90.63 s	1.63 %
Elliot RT 2	2607.68	-4.04 %	-	-
017 control	2753.05	-5.95 %	-	-

4. DISCUSSION

In the presented thesis the aim was to optimize Ca^{2+} imaging for hESC derived RPE in cell culture conditions. The hypothesis was that better Ca^{2+} imaging data could be recorded when imaging the cells in conditions as close to the physiological environment of living cells as possible, compared to imaging performed at RT.

Figure 1 shows the confocal imaging maximum intensity projection data from a 08/023 cell sample. Figure 1 A indicates the presence of the $Ca_V1.3$ channels in the samples. The Ca^{2+} ion channels are strongly centred around the primary cilia, which are specialized Ca^{2+} signalling cell organelles located on the apical side of the cells with microvilli (Delling et al. 2013). From Figure 1 B, the hexagonal shape of the RPE cells can be seen due to the stained tight junction protein ZO-1. The cell lines are clear and coherent. In Figure 1 C, actin-binding phalloidin is used to stain the actin in the RPE cytoskeleton. Actin filaments in RPE cells form bundles that give the cell its shape, internally connect the cell's adherence junctions, and form the core of the microvilli on the apical side of the cell (Tarau et al. 2019). Based on this, the phalloidin in Figure 1 C should be present everywhere in the cells, especially concentrated on the cell borders highlighting the hexagonal cell shape. In most of the cells in Figure 1 C, phalloidin does not cover the middle parts of the cell, and in certain parts of the sample, phalloidin does not properly frame the cell. The inconsistencies in the phalloidin suggest that the phalloidin did not bind to actin as intended or that there were other issues during the immunostaining process. There could also be inconsistencies in the actin cytoskeleton of the cells. According to Hongisto et al. (2017), hESC-RPE shows normal karyotypes and can be fully characterized after 9 weeks of maturation. hESC-RPE cells are usually cultured for a maximum of 11-13 weeks, after which the end-point experiments are conducted (Viheriälä et al. 2021, Johansson et al. 2019). During this thesis work, the 08/023 cells were 14-15 weeks old.

No clear spontaneous Ca^{2+} signalling data could be recorded from any of the samples except from Elliot RT 1, as can be seen in Figures 2-4. In Figure 2, both the fluorescence change seen in the cell and the intensity plot spike clearly show the spontaneous signalling occurring in the Elliot RT 1 -sample. In the Hibernate RT -sample (Figure 3), a change in fluorescence in the cell can vaguely be detected, but the intensity plot shows no clear spike. This is most likely due to the high amount of background fluorescence in the Hibernate RT Ca^{2+} imaging data. Background fluorescence can occur due to the instrumental setup or imaging solution, for example (Sun et al. 2017). Hibernate™ -A Medium is a nutrient medium and nutrients such as proteins can fluorescence themselves due to the fluorophores in their structures, which would lead to increased amounts of background when imaging. The high among of background fluorescence explains, why no clear ATP response could be visually recorded from the Hibernate RT -samples, and why the intensity plot in Figure 6 shows

changes in the intensity even before the addition of ATP. The amount of background could possibly be reduced by imaging the Hibernate -samples with a spinning-disk microscope instead of a fluorescence microscope. In spinning-disk microscopy, the excitation light is collected from a single focal plane instead of the whole sample as in fluorescence microscopy. By only collecting excitation light from a single focal plane, the effect of the disturbing background could be minimized.

Since ATP binding to its receptors triggers the release of Ca^{2+} from the intracellular Ca^{2+} storages, the addition of ATP to the sample should result in a clear ATP response that can be detected both visually and from the intensity plots. However, the only recorded ATP responses were from the Elliot RT 1 and Hibernate RT -samples. Table 3 shows the recorded relative intensities at ATP response peaks for all samples. For Elliot RT 1, the relative intensity at the ATP response peak was 14.50 %, and for Hibernate RT 31.87 %. In the case of Elliot RT 1, the ATP response can also be detected visually in Figure 5. As mentioned, no ATP response could be recorded for any of the other samples. The lack of observed ATP response and spontaneous Ca^{2+} signalling could be due to the age of the cells.

Since no spontaneous Ca^{2+} signalling data (Figure 4) or ATP response data could be recorded from the 017 control -sample either, the non-ideal condition of the 08/023 cells cannot be the only reason for the lack of Ca^{2+} imaging data. Especially in Figure 4, the series of images shows a complete lack of change in the fluorescence, as if Fluo-4 were not present in the sample. The slight fluorescence detected in the series of images is most likely due to autofluorescence instead of the fluorescent Ca^{2+} marker. Autofluorescence is the natural level of fluorescence present in living cells, which originates mostly from mitochondria and lysosomes (Monici 2005). It is possible, that the Fluo-4 stock used for this project expired during the experiments. It would explain, why Ca^{2+} imaging data could be recorded from the first measurements, but not from the following measurements conducted at a later date (see Table 3).

When dealing with Ca^{2+} imaging data, photobleaching makes comparing the recorded data between samples more difficult. In photobleaching, the light from the microscope destroys the fluorophores present in the sample (Thorley et al. 2014). This can be seen in the intensity plot in Figure 2, where the relative intensity at 60 s time point is -7.15 %. Bleach correction tools exist, but for example, the ImageJ bleach correction tool does not take the ATP spikes into account. Data with notable intensity changes is overall difficult to analyse and creating specific tools for the analysis at hand is usually necessary. In this thesis, photobleaching did not change the outcome of the results. Thus, bleach correction was not necessary. To reduce the photobleaching in the imaging phase, spinning disk microscopy could be considered instead of fluorescence microscopy. Spinning disk microscopy could yield better Ca^{2+} imaging data because of rapid multi-beam scanning, which exposes the sample to light for a reduced amount of time and thus reduces photobleaching (Gräf et al. 2005).

5. CONCLUSIONS

In this thesis, the aim was to optimize Ca^{2+} imaging for hESC-RPE in cell culture conditions. Due to the poor condition of the 08/023 cell line cells and the most likely expired Fluo-4, the experiments could not be conducted as planned. To truly optimize Ca^{2+} imaging for hESC-RPE in cell culture conditions, the experiments should be conducted again with younger cells or another cell line, such as the 08/017 cell line, and a new Fluo-4 stock. Hibernate™ -A cell nutrient medium was not suitable for Ca^{2+} imaging with a fluorescence microscope due to the high amount of background fluorescence, and therefore should be left out from later experiments. To further improve the results, fluorescence microscopy could be exchanged for spinning disk microscopy to reduce photobleaching in the samples during imaging.

REFERENCES

ABU KHAMIDAKH, A., 2019. Assessment of Ca2+ Dynamics in Human Retinal Pigment Epithelial Cell Cultures. Tampere University.

ALBERTS, B., JOHNSON, A., LEWIS, J. et al., 2015. Molecular Biology of the Cell. 6th ed. New York, US: Garland Science.

BOOTMAN, M.D., 2012. Calcium signaling. Cold Spring Harbor Perspectives in Biology, July 1, vol. 4, no. 7, pp. e011171. DOI 10.1101/cshperspect.a011171.

DELLING, M., DECAEN, P.G., DOERNER, J.F. et al., 2013. Primary cilia are specialized calcium signaling organelles. Nature, December 12, vol. 504, no. 7479, pp. 311-314. DOI 10.1038/nature12833.

GEE, K.R., BROWN, K.A., CHEN, W.U. et al., 2000. Chemical and physiological characterization of fluo-4 Ca2+-indicator dyes. Cell Calcium, February 1, vol. 27, no. 2, pp. 97-106. DOI 10.1054/ceca.1999.0095.

GRÄF, R., RIETDORF, J. and ZIMMERMANN, T., 2005. Live cell spinning disk microscopy. Advances in Biochemical Engineering/Biotechnology, pp. 57-75. DOI 10.1007/b102210.

HONGISTO, H., ILMARINEN, T., VATTULAINEN, M. et al., 2017. Xeno- and feeder-free differentiation of human pluripotent stem cells to two distinct ocular epithelial cell types using simple modifications of one method. Stem Cell Research & Therapy, December 29, vol. 8. DOI 10.1186/s13287-017-0738-4.

JOHANSSON, J.K., KAREMA-JOKINEN, V.I., HAKANEN, S. et al., 2019. Sodium channels enable fast electrical signaling and regulate phagocytosis in the retinal pigment epithelium. BMC Biology, August 15, vol. 17, no. 1, pp. 63. DOI 10.1186/s12915-019-0681-1.

KEW, J.N.C. and KEMP, J.A., 2005. Ionotropic and metabotropic glutamate receptor structure and pharmacology. Psychopharmacology, April, vol. 179, no. 1, pp. 4-29. DOI 10.1007/s00213-005-2200-z.

KORKKA, I., VIHERIÄLÄ, T., JUUTI-UUSITALO, K. et al., 2018. Functional Voltage-Gated Calcium Channels Are Present in Human Embryonic Stem Cell-Derived Retinal Pigment Epithelium. STEM CELLS Translational Medicine, November 04, pp. 179-193. DOI 10.1002/sctm.18-0026.

LAKKARAJU, A., UMAPATHY, A., TAN, L.X. et al., 2020. The cell biology of the retinal pigment epithelium. Progress in Retinal and Eye Research, September 1, vol. 78, pp. e100846. DOI 10.1016/j.preteyeres.2020.100846.

MONICI, M., 2005. Cell and tissue autofluorescence research and diagnostic applications. Biotechnology Annual Review Elsevier, January 1, pp. 227-256. DOI 10.1016/S1387-2656(05)11007-2.

SALCEDA, R. and RIESGO-ESCOVAR, J.R., 1990. Characterization of calcium uptake in chick retinal pigment epithelium. Pigment Cell Research, September, vol. 3, no. 3, pp. 141-145. DOI 10.1111/j.1600-0749.1990.tb00278.x.

SKOTTMAN, H., 2010. Derivation and characterization of three new human embryonic stem cell lines in Finland. In Vitro Cellular & Developmental Biology - Animal, February 23, vol. 43, pp. 206-209. DOI 10.1007/s11626-010-9286-2.

STRAUSS, O., 2005. The retinal pigment epithelium in visual function. Physiological Reviews, July, vol. 85, no. 3, pp. 845-881. DOI 10.1152/physrev.00021.2004.

SUN, Y., IP, P. and CHAKRABARTTY, A., 2017. Simple Elimination of Background Fluorescence in Formalin-Fixed Human Brain Tissue for Immunofluorescence Microscopy. Journal of Visualized Experiments, September 3, no. 127, pp. e56188. DOI 10.3791/56188.

TARAU, I., BERLIN, A., CURCIO, C.A. et al., 2019. The Cytoskeleton of the Retinal Pigment Epithelium: from Normal Aging to Age-Related Macular Degeneration. International Journal of Molecular Sciences, July 22, vol. 20, no. 14. DOI 10.3390/ijms20143578.

THORLEY, J.A., PIKE, J. and RAPPOPORT, J.Z., 2014. Chapter 14 - Super-resolution Microscopy: A Comparison of Commercially Available Options. Fluorescence Microscopy Boston, January 1, pp. 199-212.

VIHERIÄLÄ, T., SORVARI, J., IHALAINEN, T.O. et al., 2021. Culture surface protein coatings affect the barrier properties and calcium signalling of hESC-RPE. Scientific Reports, January 13, vol. 11, no. 1, pp. 1-14. DOI 10.1038/s41598-020-79638-8.